Oncogene (2016), 1–10

www.nature.com/onc

ORIGINAL ARTICLE

Sensitization of retinoids and corticoids to epigenetic drugs in MYC-activated lung cancers by antitumor reprogramming

OA Romero[1,5], S Verdura[1,5], M Torres-Diz[1], A Gomez[2], S Moran[2], E Condom[3], M Esteller[2], A Villanueva[4] and M Sanchez-Cespedes[1]

Components of the SWI/SNF chromatin remodeling complex, including BRG1 (also SMARCA4), are inactivated in cancer. Among other functions, SWI/SNF orchestrates the response to retinoid acid (RA) and glucocorticoids (GC) involving downregulation of MYC. The epigenetic drugs SAHA and azacytidine, as well as RA and GC, are currently being used to treat some malignancies but their therapeutic potential in lung cancer is not well established. Here we aimed to determine the possible therapeutic effects of azacytidine and SAHA (A/S) alone or in combination with GC plus RA (GC/RA) in lung cancers with either *BRG1* inactivation or *MYC* amplification. *In vitro*, responses to GC/RA treatment were more effective in *MYC*-amplified cells. These effects were mediated by BRG1 and involved a reprogramming towards prodifferentiation gene expression signatures and downregulation of MYC. In *MYC*-amplified cells, administration of GC/RA enhanced the cell growth inhibitory effects of A/S which, in turn, accentuated the prodifferentiation features promoted by GC/RA. Finally, these treatments improved overall survival of mice orthotopically implanted with *MYC*-amplified, but not *BRG1*-mutant, cells and reduced tumor cell viability and proliferation. We propose that the combination of epigenetic treatments with retinoids and corticoids of MYC-driven lung tumors constitute a strategy for therapeutic intervention in this otherwise incurable disease.

Oncogene advance online publication, 5 September 2016; doi:10.1038/onc.2016.296

INTRODUCTION

The widespread occurrence of alterations at genes encoding different components of the SWI/SNF complex reveals an important new feature that sustains cancer development and offers novel potential strategies for cancer therapeutics.[1,2] We discovered that in lung cancer the SWI/SNF component, *BRG1* (also called *SMARCA4*), is genetically inactivated in about 30% of non-small cell lung cancers and occurs in a background of wild-type *MYC* (*C*, *L* or *N*).[3–5] More recently, we noted tumor-specific inactivation of the MYC-associated factor X gene, *MAX*, in about 10% of small cell lung cancers, where it is present in tumors that are wild type for *MYC* and *BRG1*.[6] Altogether, the genetic observations coupled with functional studies[5–8] indicate the existence of an important network, involving SWI/SNF and MAX/MYC that is critical to lung cancer development.

The SWI/SNF chromatin-remodeling complex modifies the structure of the chromatin by the ATP-dependent disruption of DNA–histone interactions at the nucleosomes to activate or repress gene expression.[9,10] In healthy adults and during embryonic development, the complex is involved in the control of cell differentiation and in tissue specification.[11–13] The effect of the SWI/SNF complex on some of these processes is, at least in part, related to its involvement in regulating hormone-responsive promoters. Components of the SWI/SNF complex bind to various nuclear receptors, such as those of estrogen, progesterone, androgen, glucocorticoids (GCs) and retinoic acid (RA), thereby adapting the gene expression programs to the demands of the cell environmental requirements.[14–18]

RA and GC are well-known modulators of cell differentiation, embryonic development and morphogenesis[19] and are used therapeutically to treat some types of cancers. GC are part of the curative treatment of acute lymphoblastic leukemia while RA is the therapeutic agent for some neuroblastomas and acute promyelocytic leukemia, which both carry the promyelocytic leukemia–RA receptor alpha gene fusion.[20–22] GC are also used as a comedication to reduce side effects in cancer treatment.[23] However, most solid tumors, including lung cancers, are refractory to GC- and RA-based therapies. Underlying some cases of refractoriness to GC and RA is a dysfunctional SWI/SNF complex, for example, owing to alterations at BRG1.[5,24]

On the other hand, compounds that modulate the structure of the chromatin and promote gene transcription by increasing DNA accessibility are currently used to treat cancer. These include histone deacetylase (HDAC) inhibitors, in hematological malignancies and cutaneous T-cell lymphomas, and inhibitors of DNA methylation such as azacytidine for myelodysplasic syndrome.[25] These drugs have been tested in non-small cell lung cancer (NSCLC) patients in two studies, in which they showed no major responses.[26,27] However, in a phase I/II trial, the combination of the two inhibitors produced a median survival of the entire cohort that was significantly longer than those of the existing therapeutic options.[28]

Using lung cancer as a model, we aimed to determine the possible therapeutic effects of HDACs and DNA methylation

[1]Genes and Cancer Group, Cancer Epigenetics and Biology Program (PEBC), Bellvitge Biomedical Research Institute-IDIBELL, Barcelona, Spain; [2]Cancer Epigenetics Groups, Cancer Epigenetics and Biology Program (PEBC), Bellvitge Biomedical Research Institute-IDIBELL, Barcelona, Spain; [3]Pathology Department, Bellvitge Hospital, Barcelona, Spain. and [4]Translational Research Laboratory, Catalan Institute of Oncology (ICO), Bellvitge Biomedical Research Institute-IDIBELL, Barcelona, Spain. Correspondence: Dr M Sanchez-Cespedes, Genes and Cancer Group, Cancer Epigenetics and Biology Program (PEBC), Bellvitge Biomedical Research Institute (IDIBELL), Hospital Duran i Reynals, Av Gran Via de l'Hospitalet, 199-203, Hospitalet de Llobregat, Barcelona 08908, Spain.
E-mail: Spain.mscespedes@idibell.cat
[5]These authors contributed equally to this work.
Received 4 January 2016; revised 6 July 2016; accepted 15 July 2016

inhibitors alone or in combination with retinoids and corticoids and whether the status of the *BRG1* and *MYC* genes predicts sensitivity to these treatments.

RESULTS

GCs and retinoids sensitize HDAC and DNA methylation inhibitors to reduce cell growth in AmpMYC/wtBRG1 lung cancer cells

We had previously shown that *BRG1* is required to respond to GC and RA.[5] Here we further investigated the requirement for BRG1 to achieve responses to combined GC and RA (hereafter GC/RA) in lung cancer. We also wondered whether the DNA methylation inhibitor, azacytidine, or the HDAC inhibitor, SAHA, could be a substitute for the activity of BRG1 in cells with inactivated *BRG1*. First, we observed that, as compared with the single administration, the simultaneous treatment of azacytidine and SAHA enhanced the effects in decreasing cell growth in various lung cancer cells (Supplementary Figure S1a). An isobologram analysis of drug interactions in two of the cell lines determined that this effect was synergic (Figure 1a). This agrees with previous observations showing that combining A/S resulted in clinical responses in NSCLC patients, as opposed to the lack of effect of each drug when administered individually.[26–28] Furthermore, GC/RA enhanced the growth-inhibitory effect of azacytidine and SAHA combined (hereafter A/S) in the H460 cell line (Supplementary Figure S1b). Altogether, the published data and

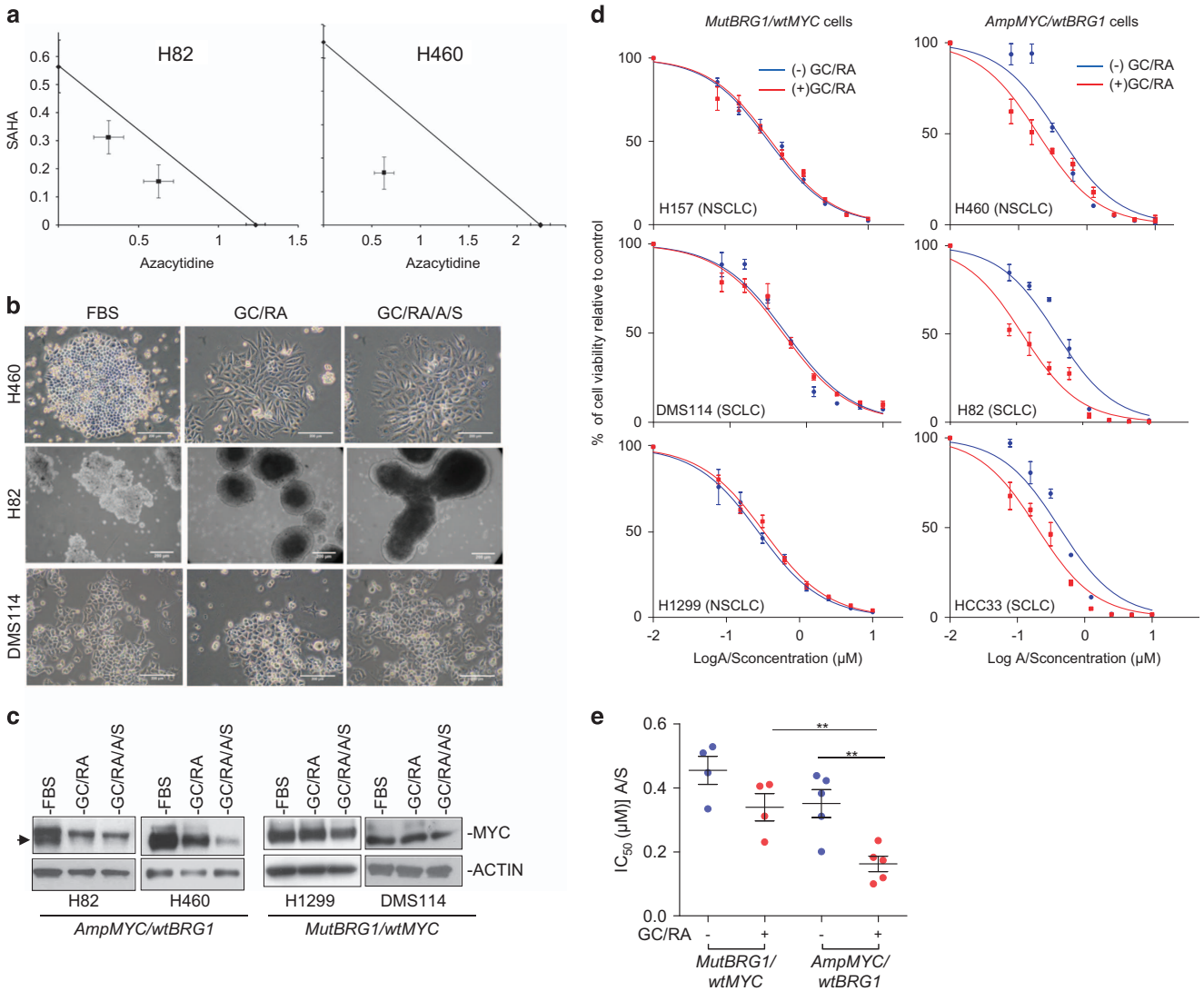

Figure 1. GC/RA and A/S reduce growth of *MYC*-amplified cancer cells and the effects are enhanced with the dual combination. (**a**) Isobolograms at IC_{50} of the indicated cells. The solid line joins the IC_{50} for azacytidine and SAHA as single agents and shows the point at which additivity would occur. Data points, represented by dots located below the line with the 95% confidence limits as error bars, indicate synergy. (**b**) Phase-contrast images of the indicated cells untreated (fetal bovine serum (FBS)) or treated with GC/RA (1 μM each) or GC/RA plus A/S (0.2 μM each) for 5 days. The appearance of the H82 cells change from tight cell aggregation to large floating spheroids upon treatment with GC/RA. Scale bar, 200 μm. (**c**) Western blotting depicting the levels of MYC in the indicated cells and treatments. β-ACTIN, protein-loading control. The black arrow points to the specific bands corresponding to the MYC protein in the H82 cells. The upper band is non-specific. (**d**) Cell viability of the indicated cell lines, measured using MTT assays, after treatment with increasing concentrations of A/S with (+) or without (−) GC/RA (2.5 μM each) for 5 days. This concentration was chosen because it was higher than the mean IC_{50} for GC/RA in the AmpMYC/wtBRG1 cells. Lines show the number of viable cells relative to the untreated cells. Information about the histopathology of each cell lines is also indicated. (**e**) Distribution and mean of the IC_{50} for the A/S with (+) and without (−) GC/RA (2.5 μM each) for the indicated group of cells (Supplementary Table S1). $^{**}P < 0.01$, two-tailed Student's *t*-test.

our preliminary observations prompted us to explore this further. We used tumor-derived cell lines that have proved to be effective systems for establishing the link between specific tumor genotypes and the response to molecularly targeted drugs.[29]

Previously, we had shown that genetic inactivation of *BRG1* is mutually exclusive with amplification of the *MYC* genes, which is consistent with a biological connection between these two cancer proteins.[3] Taking this into account, we selected nine lung cancer cell lines that were either mutant for *BRG1* and wild type for *MYC* (hereafter *MutBRG1/wtMYC*) or wild type for *BRG1* and amplified at any of the *MYC*-family genes (hereafter *AmpMYC/wtBRG1*) (Supplementary Table S1).

The treatment with GC/RA triggered phenotypic modifications and slightly reduced the levels of MYC in the *AmpMYC/wtBRG1* cells, and these effects were also strongly enhanced by addition of A/S (Figures 1b and c; Supplementary Figure S2). The downregulation of MYC in cells carrying *MYC*, *MYCN* and *MYCL* amplification is possible because, in these cell lines, the amplicon contains the 5′-untranslated region with the P1 and P2 promoters (http://www.sanger.ac.uk/), responsible for the MYC-negative autoregulatory mechanism.[30,31] In marked contrast, the *MutBRG1/wtMYC* cells, with the single exception of the A549 cells, underwent only subtle or no changes in morphology or in the levels of MYC after treatment with GC/RA, regardless of whether A/S was coadministered (Supplementary Figure S2).

Next we calculated the half maximal inhibitory concentration (IC_{50}) for A/S with or without coadministration of GC/RA to assess the effects of these treatments on cell growth. The values of IC_{50} for the A/S treatment were lower in *AmpMYC/wtBRG1* cells, although the differences did not reach statistical significance (Figures 1d and e). The combination with GC/RA significantly reduced the IC_{50} of each treatment in the *AmpMYC/wtBRG1* cells (Figures 1d and e).

Depletion of BRG1 in AmpMYC/wtBRG1 cells impairs responses to treatments with GC/RA and the combination with azacytidine and SAHA

Next we depleted BRG1 in *AmpMYC/wtBRG1* cells using two different shBRG1 (shBRG1#1 and shBRG1#4), previously validated by our group[5–6] (Figure 2a; Supplementary Figure S3a). In accordance with our previous results,[5] the depletion of BRG1 markedly reduced the ability of the cells to undergo changes in morphology following treatment with GC/RA and GC/RA combined with A/S (Figure 2b; Supplementary Figure S3b). The depletion of BRG1 also decreased the capability of the cells to decrease cell growth in response to GC/RA combined with A/S (Figures 2c and d; Supplementary Figure S3c). Overall, these observations imply that the response to GC/RA is strongly dependent on the presence of BRG1.

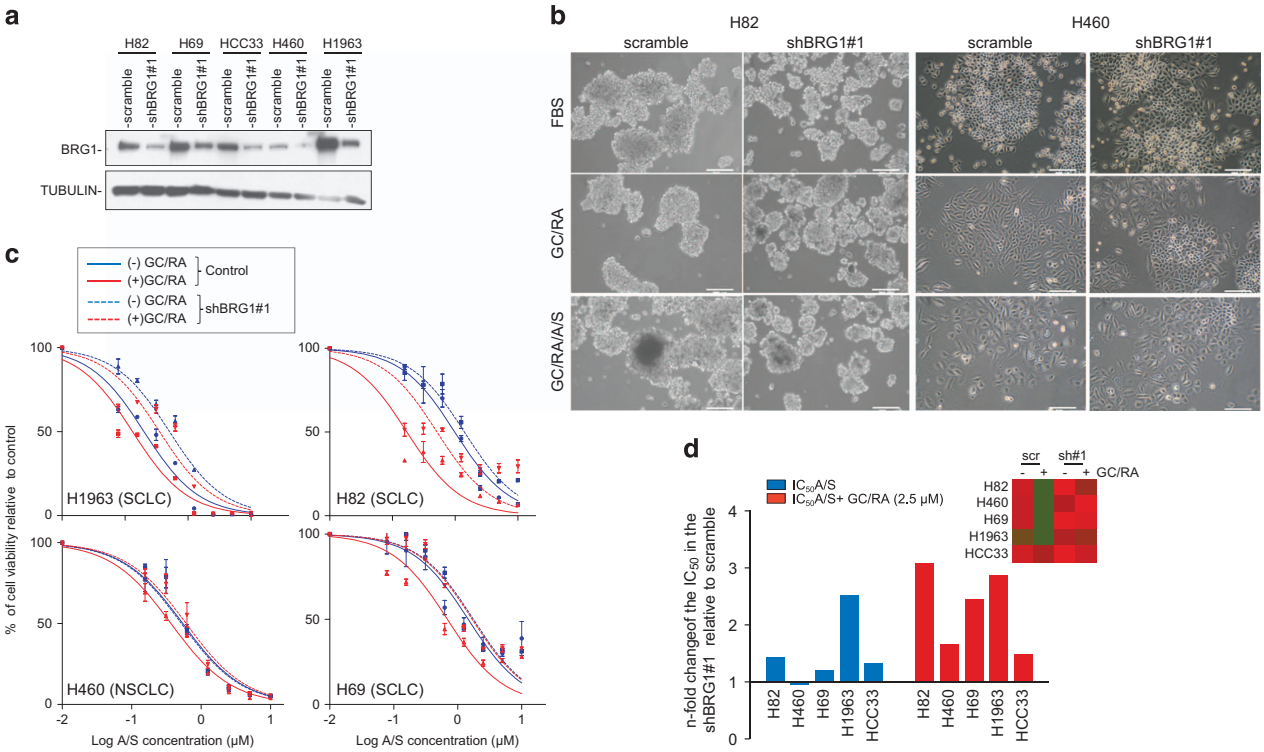

Figure 2. Depletion of BRG1 using shBRG1 reverted the growth inhibition effects in response to GC/RA and to GC/RA/A/S of *MYC*-amplified lung cancer cell lines. (**a**) Western blotting depicting the downregulation of BRG1 protein levels, using shRNAs (shBRG1#1) targeting BRG1 (from Romero *et al.*[5]) in the indicated cell lines. TUBULIN, protein-loading control. Scramble shRNAs (scramble) were used as control. (**b**) Phase-contrast images of the H82 and H460 cells, with downregulated expression of BRG1 (shBRG1#1), and of the scramble control cells, after treatment with GC/RA (1 μM each) or GC/RA plus A/S (0.2 μM each) for 5 days. Untreated cells (fetal bovine serum (FBS)) were included as a control. Scale bar, 200 μm. (**c**) Assessment of cell viability, measured using MTT assays, after treatment with increasing concentrations of A/S, with (+) or without (−) GC/RA (2.5 μM each), for 5 days, after downregulating the expression of BRG1 (shBRG1#1), and of the scramble control cells. Lines represent the number of viable cells relative to the untreated cells. Error bars, ±s.d. from three replicates. (**d**) *n*-Fold change of the IC_{50} of A/S treatment with and without GC/RA (2.5 μM each) after downregulating BRG1 expression with shBRG1#1, relative to scramble control cells, in the indicated cell lines. Inset, heatmap with the logIC_{50} values of the A/S treatment with (+) and without (−) GC/RA(2.5 μM each).Scr, scramble control; sh#1, shBRG1#1.

The ability to activate the expression of prodifferentiation genes underlies the sensitivity to GC/RA-based treatments in AmpMYC/wtBRG1 lung cancer cells

To explore in depth the molecular features that underlie the sensitivity and refractoriness to the GC/RA-based treatment, we compared the gene expression and DNA methylation profiles of various cancer cells before and after treatments with GC/RA or with A/S plus GC/RA (hereafter GC/RA/A/S). We also determined the changes in gene expression and DNA methylation before and after depleting the *BRG1* expression.

Unsupervised hierarchical clustering of the 10 000 most dynamic probes segregated cell lines on the basis of cell identity and histopathology (Supplementary Figure S4a). This was expected because gene expression patterns in lung cancer are strongly influenced by the histopathology, which mirrors the cell of origin.[32–33] Administration of GC/RA triggered more than twofold changes in the expression of hundreds of genes in all but the DMS114 and H1299 cells, which were barely affected by the treatment (Figure 3a; Supplementary Tables S2–S6). In all the cell lines, the changes in gene expression triggered by GC/RA were enhanced after the addition of A/S (Figures 4a and b). Notably, most of the genes that were upregulated after these treatments were expressed at low levels in the untreated cells, suggesting a switch of the mechanism of activation of silenced genes (Figure 3b).

Analysis of gene functionalities showed that GC/RA upregulated genes involved in cell differentiation and development, especially in *AmpMYC/wtBRG1* cells. For example, the H82 cells showed an increase of neural- and retina-related genes, implying a neuroendocrine origin for the SCLC and its similarity to cells from the

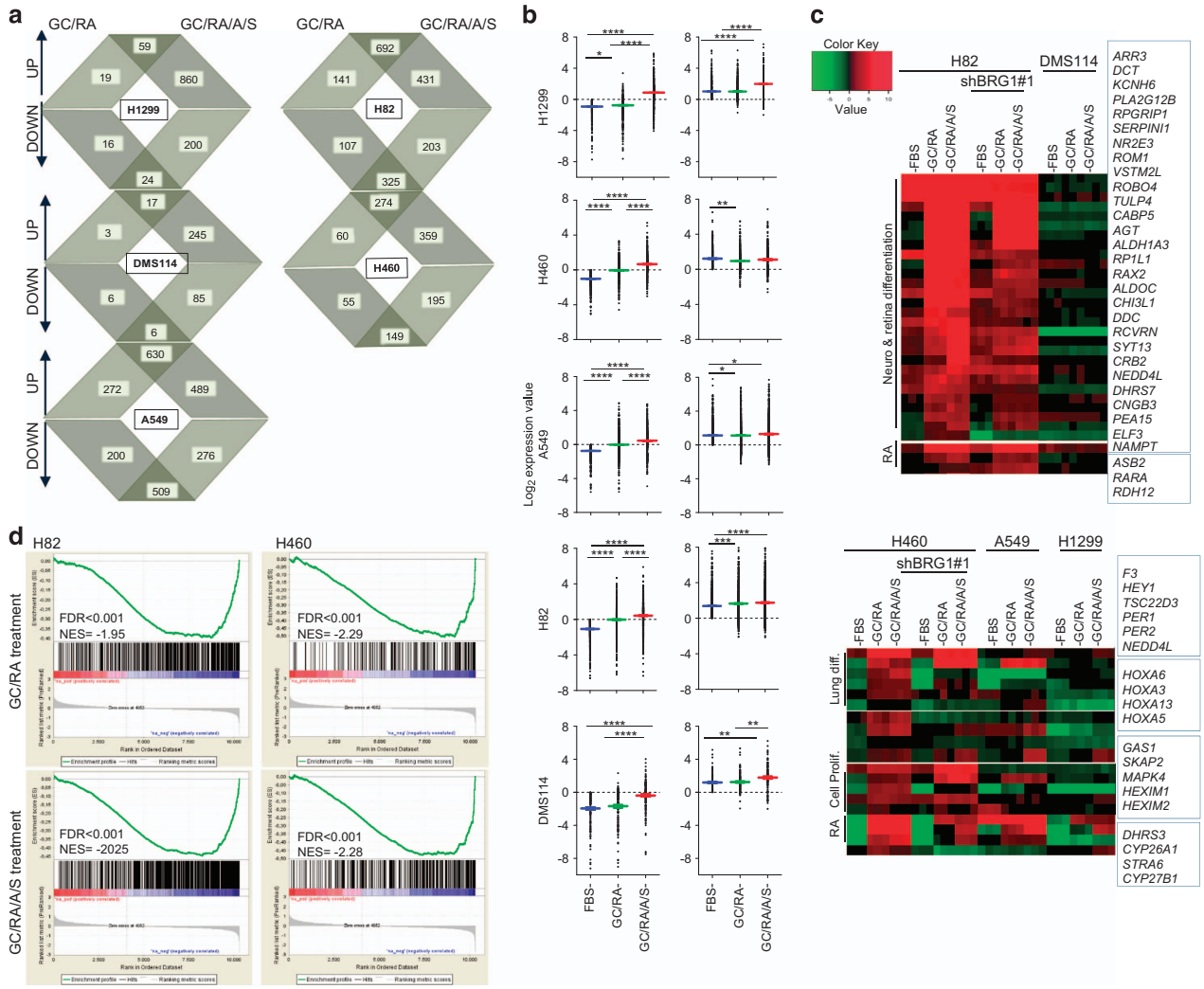

Figure 3. GC/RA triggers prodifferentiation gene expression signatures in *MYC*-amplified lung cancer cell lines and these responses are enhanced by A/S and depend on an active BRG1. (**a**) Venn diagram of differential gene expression overlap after treatment with GC/RA and GC/RA/A/S, relative to untreated cells, in each of the five indicated cell lines. The upper and lower halves of each diagram illustrate the upregulated (UP) and downregulated (DOWN) genes, respectively. (**b**) Aligned dot plot in each indicated cell line and treatment. Each dot represents the expression values from the lists of genes that are at least twofold upregulated or downregulated after administration of GC/RA/A/S. Left panels, genes with expression values of < 0 in the untreated cells (fetal bovine serum (FBS)) are included; right panels, only genes with expression values of > 0 are included. The means are indicated in each case. $^{*}P < 0.05$; $^{**}P < 0.01$; $^{***}P < 0.005$; $^{****}P < 0.001$ two-tailed Student's *t*-test. (**c**) Heatmap of the selected genes upregulated at least twofold upon administration of the indicated treatments. Transcripts from the various indicated functions have been selected. The heatmap also includes the values of gene expression levels after downregulation of BRG1 expression (shBRG1#1). (**d**) Graph of the ranked gene lists derived from the comparison (using GSEA) of data set GSE6077 and gene lists. Genes upregulated by the indicated treatments vs data set GSE6077 as reference. Data set GSE6077: lungs from ED 18.5 transgenic mice overexpressing Nmyc in the lung epithelia vs normal controls. Probabilities and false-discovery rates (FDRs) are indicated.

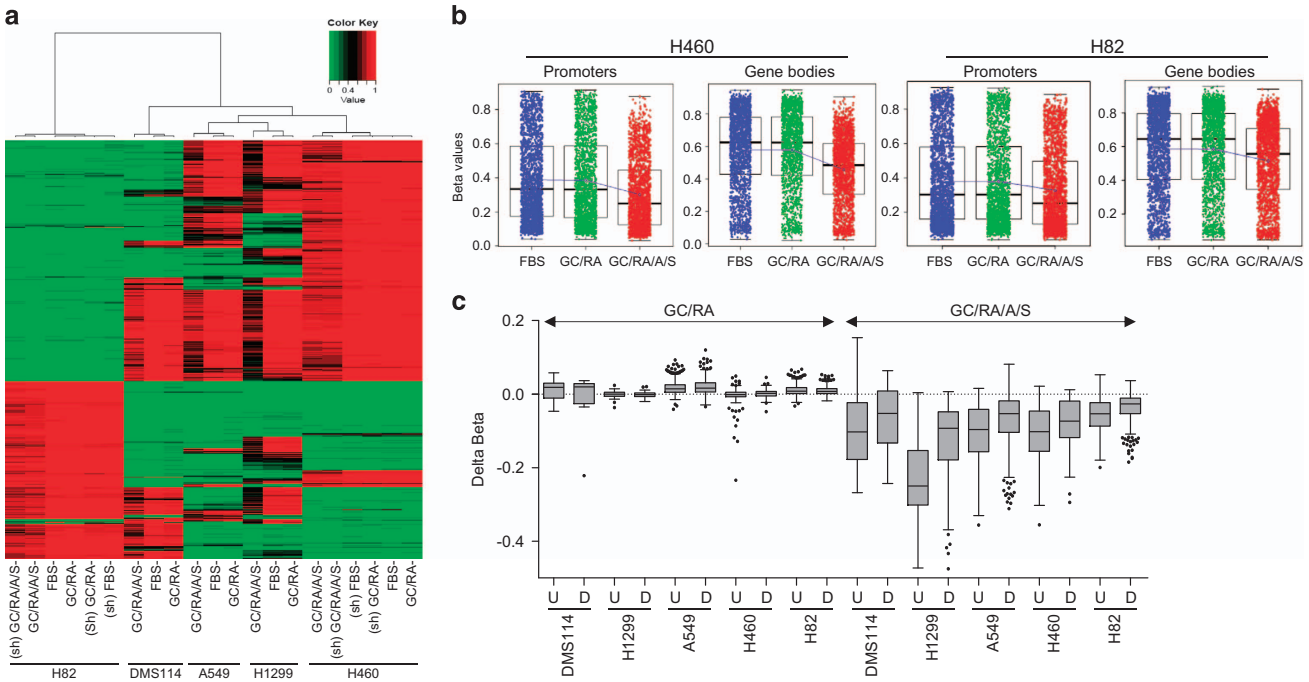

Figure 4. Analysis of the changes in genome-wide methylation, using a 450 000 CpG methylation microarray, after the GC/RA and GC/RA/A/S treatments. (**a**) Unsupervised hierarchical clustering, in the indicated cell lines and treatments, for the 4855 most variable CpGs. The heatmap colors illustrate beta values representing the degree of methylation from low (green) to high (red), as shown by the scale at the top-right of the figure. (sh), refers to shBRG1. (**b**) Scatter plots showing the beta values of the CpGs at the promoters or bodies of selected groups of genes in the untreated cells (fetal bovine serum (FBS)) and after the indicated treatments in the H82 and H460 lung cancer cell lines. (**c**) Box plot showing changes in mean beta values in CpG promoters of the genes upregulated (U) and downregulated (D).

retina (Figure 3c; Supplementary Figure S4b).[19,34] Likewise, the treatment with GC/RA in the H460 cells upregulated genes involved in developmental processes and in the negative control of cell proliferation. These included lung-specific transcripts (for example, *F3*, *HEY1*) (http://biogps.org) and *HOX*-related genes, which are the targets of RA (Figure 3c; Supplementary Figure S4b).[19,35] Consistent with the reduction in levels of MYC, the expression profile of upregulated genes after GC/RA and GC/RA/A/S treatments in H82 and H460 cells was inversely associated with the profile of mice embryonic lungs overexpressing Nmyc and Cmyc (Figure 3d; Supplementary Figure S5). As expected, the depletion of BRG1 in these cells attenuated the increase in gene expression triggered by GC/RA and GC/RA/A/S (Figure 3c; Supplementary Figure S6).

Regarding the *MutBRG1/wtMYC* cells, the administration of GC/RA and GC/RA/A/S in the DMS114 and H1299 cells did not trigger gene expression profiles compatible with cell differentiation functionalities. It is of particular note that in the A549 cells the response to GC/RA involved changes in the expression of hundreds of genes, including transcripts related to cell differentiation (Figure 3a; Supplementary Figure S5b). This is consistent with the aforementioned changes in morphology that this cell line undergoes upon treatment with GC/RA, indicating some responsiveness to these compounds (Figure 1a; Supplementary Figure S2). As these cells are derived from a well-differentiated lung adenocarcinoma, the structure of the chromatin of these cells in most RA- and GC-responsive promoters may already be accessible and may not require SWI/SNF activity.

To determine whether these gene expression changes were associated with modifications in DNA methylation, we performed genome-wide DNA methylation profiling.[36,37] We identified 4855 CpGs with the most variable methylation levels that were plotted in an unsupervised manner (Figure 4a). Similar to the gene expression profiles, methylation profiles also discriminated cell identity. The GC/RA treatment did not change global methylation or the levels of CpG methylation at the promoters of genes upregulated and downregulated after GC/RA treatment. In contrast, the coadministration of A/S reduced overall methylation by 15–20% in all cell lines of CpGs in gene promoters and bodies, presumably by the action of azacytidine (Figure 4b). The reduction of CpG methylation, by A/S, in gene promoters was more pronounced in the group of upregulated genes, associating demethylation with the re-expression of these genes (Figure 4c).

MYC amplification predicts sensitivity to GC/RA, alone or in combination with other drugs, in *in vivo* models

We investigated the ability of GC/RA, A/S and GC/RA/A/S in suppressing tumor growth *in vivo*. To this end, the A549, H82, H460 and H1299 cell lines were grown orthotopically in the lung parenchyma of nude mice.[5,38] The animals, implanted with the cell lines, were randomly assigned to the four treatment groups of 8–10 mice as follows: group 1, vehicle control; group 2, treated with GC/RA; group 3 treated with A/S; and group 4 treated with GC/RA/A/S. Cisplatin-based treatments were administered in group 5, treated with cisplatin alone; and in group 6, treated with cisplatin plus GC/RA. Although all the treatments were well tolerated by the mice, the administration of GC/RA reduced the weight of the animals, recovering after 2–3 days without treatment.

First, we examined the ability of the different treatments to affect overall survival. Compared with the control group, treatment with GC/RA increased overall survival of the animals implanted with the *AmpMYC/wtBRG1* cells, H82 and H460, although in the latter type only when cotreated with cisplatin (Figure 5; Supplementary Figure S7a). None of the treatments significantly improved overall survival in animals implanted with the *MutBRG1/wtMYC* cells. Histopathological examination revealed significantly higher rates of necrosis in tumors from animals

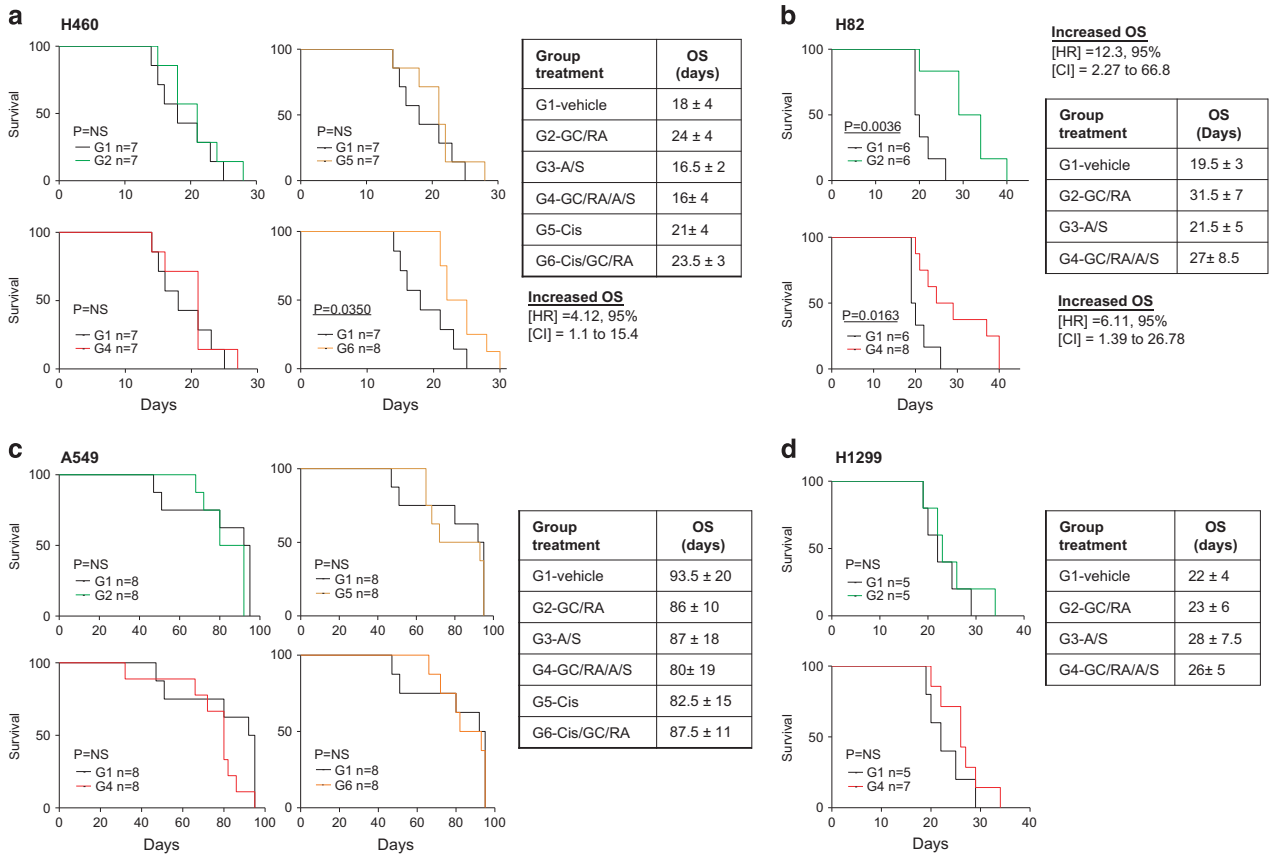

Figure 5. *MYC* amplification predicts sensitivity to GC/RA, alone or in combination with other drugs, in mice orthotopic models of lung cancer. Kaplan–Meier curves showing overall survival (OS) probability for each treatment (G2, G4, G5 and G6) compared with that for the vehicle control group (G1). The lung cell line implanted in each case and the number of mice in each group (*n*) are indicated. HR, hazard ratio; CI, 95% confidence interval. (**a**) H460, (**b**) H82, (**c**) A549 and (**d**) H1299 cell line. *P*-values from the log-rank (Mantel–Cox) tests of the plots are included. NS, not significant. Panels on the right show the mean ± s.d. survival time for the different groups of treatments. Cis, cisplatin. The G1 vs G3 and G1 vs G5 plots for the rest of cell lines are included in Supplementary Figure S7.

treated with GC/RA only in mice implanted with *AmpMYC/wtBRG1* cells (Figures 6a and b; Supplementary Figure S7b). Likewise, we analyzed the levels of induced cleavage at poly-(ADP-ribose) polymerase 1 (PARP1) and caspase 3, as surrogate markers for apoptosis, and the levels of Ki67, as a surrogate marker for cell proliferation. A significant increase in apoptosis and a reduction in cell proliferation were evident after treatment with GC/RA specifically in tumors exhibiting *MYC* amplification (Figures 6c–e).

DISCUSSION

RA and GC have important roles in normal lung development. In mouse models, a deficiency of RA induces squamous metaplasia and the addition of RA can effect regression of premalignant lesions.[39,40] It is also well established the importance of GCs in perinatal lung development.[41,42] However, these compounds have therapeutic effects on some childhood and hematological malignancies[20–22] but not in lung cancer or most solid tumors.[42,43]

There is a physical interaction between components of the SWI/SNF complex and the RA and GC receptors and there is evidence of nucleosome-disrupting activity of the complex to allow transcription mediated by RA and GC receptors.[15,17,21] Here we report that inactivation of *BRG1* confers refractoriness to the enhanced growth-inhibitory effects triggered by GC/RA during A/S treatment *in vitro*, whereas amplification at any of the *MYC* genes predicts sensitivity. The sensitization to A/S treatment triggered by GC/RA also involved a reduction in MYC levels and global transcriptional changes, compatible with reprogramming towards cell differentiation. Downregulation of *MYC* following GC or RA treatment is well established,[44,45] but here we report that this effect is enhanced by A/S and is more effective in *MYC*-activated cells. A MYC-negative autoregulatory mechanism that is mediated by the SWI/SNF complex would explain the refractoriness of most *BRG1*-mutant cells.[5,46] Taking all the above into account, we believe that the sensitization to A/S by GC/RA requires the nucleosome-disrupting activity of the SWI/SNF complex containing BRG1.

Here we have focused on the genetic status of the *MYC* genes and of *BRG1* and have eluded the comparison among histopathologies. *BRG1* mutations are significantly more common in NSCLC, whereas amplification of the *MYC* genes, especially *NMYC* and *LMYC*, predominates in SCLC.[3] We have included an SCLC cell line, the DMS114, with inactivation at *BRG1* and a NSCLC cell line, the H460, with *MYC* amplification. The DMS114 cells were refractory and the H460 cells were sensitive to the treatments, supporting that the genetic background is the main determinant of the response to these treatments. In spite of these observations, we believe that additional studies are needed to determine the influence of the lung cancer histopathologies in the response to these compounds.

Malignancies currently treated with GC or RA often have genetically activated MYC. Such is the case for neuroblastomas, with *NMYC* amplification, and Burkitt lymphoma, which is

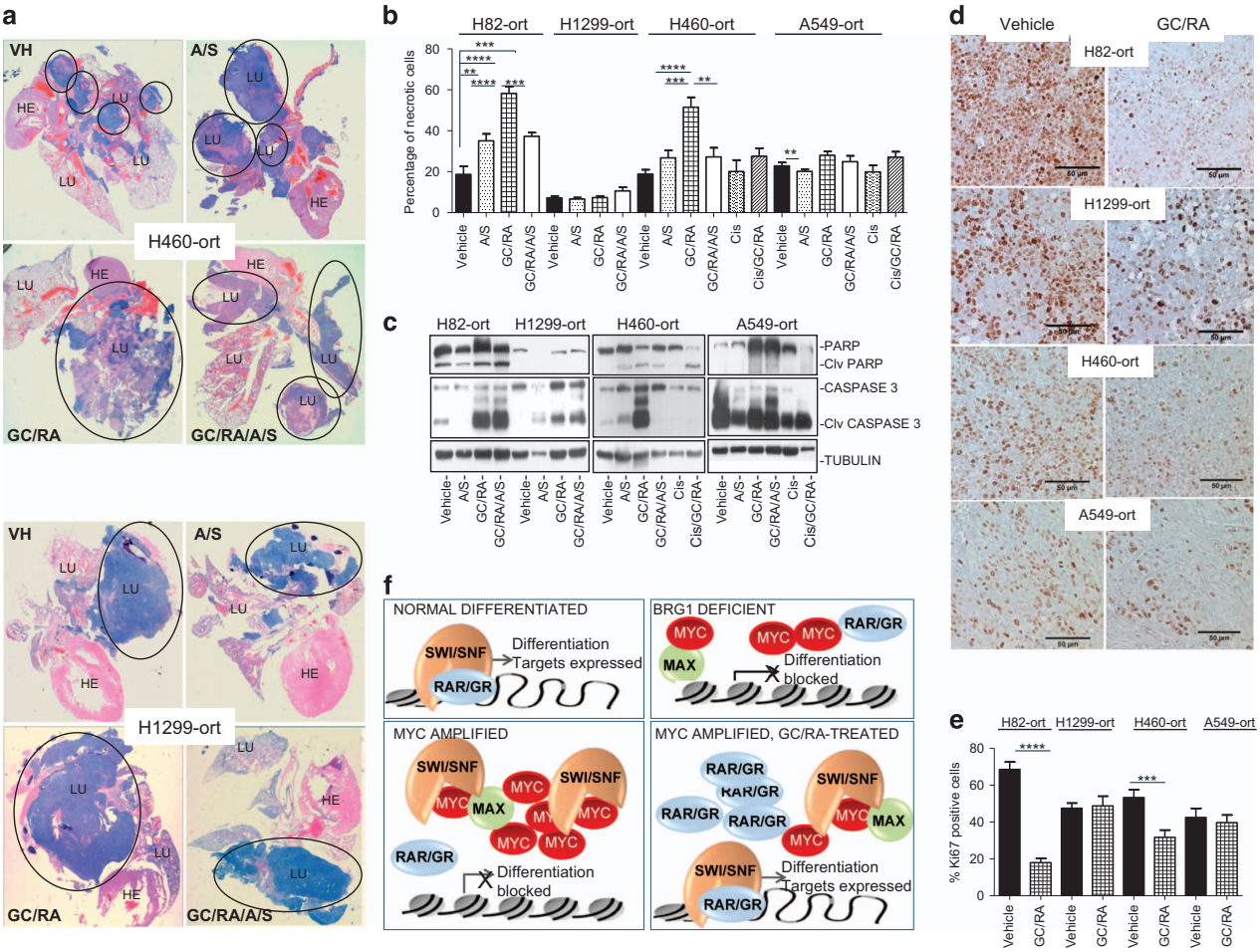

Figure 6. GC/RA treatment has a strong effect on increasing cell death of *MYC*-amplified lung cancer cells in *in vivo* orthotopic (ort) models. (**a**) Representative sections of the hematoxylin and eosin staining of the tumors (dark blue in circles) from the AmpMYC/wtBRG1, H460, and the *MutBRG1/wtMYC*, H1299, cells treated with the indicated treatments or vehicle (VH). The treatments were initiated from 8 to 10 days after tumor implantation. The pink areas inside the tumors are indicative of necrosis. HE, heart; LU, lung. (**b**) Quantification of the necrotic areas. Error bars show s.e.m. across nine replicates. (**c**) Western blotting depicting the cleavage of PARP and CASPASE-3 in the orthotopic tumors from the indicated cells, following the different treatments or vehicle. TUBULIN, protein-loading control. (**d**) Representative Ki67 immunostaining of the indicated cells. Scale bar, 50 μm. (**e**) Quantification of Ki67-positive cells. Error bars show s.e.m. across nine replicates. $^{**}P < 0.01$; $^{***}P < 0.005$; $^{****}P < 0.001$: two-tailed Student's *t*-test. (**f**) Proposed model, representing the activity of the glucorticoid and retinoic acid receptors (GR and RAR, respectively) in four different scenarios. In a normal differentiated cell, the levels of MYC are low and the SWI/SNF complex binds GR and RAR leading to relaxation of chromatin structure to increase transcription of GR- and RAR-target genes. In the *BRG1*-inactivated cancer cells, the SWI/SNF complex is not active, whereas, in the *MYC*-amplified cells, there is a strong overexpression of MYC molecules that compete with GR and RAR for binding to the complex. In both cases, the chromatin, at the RAR and GR-target promoters, is closed and inaccessible. In contrast to the *BRG1* mutants, in the *MYC*-amplified cells the sensitiveness to GC/RA can be restored by treating with supra-physiological levels of GC/RA. This will increase RAR and GR activity and downregulate MYC, counteracting the balance toward a more abundant RAR and GR. Although it is not depicted in this model, the simultaneous administration of A/S would enhance the activity of the SWI/SNF complex in those promoters.

associated with translocations involving *MYC*.[20–22] Furthermore, the BET bromodomain inhibitor JQ1, which triggers the down-regulation of MYC, has antiproliferative effects in those multiple myeloma cells and neuroblastomas that carry *MYC* translocations and *MYCN* amplification, respectively.[47] Taking into account that activated oncogenes are an Achilles heel for most cancer cells, a treatment that triggers *MYC* downregulation may be expected to be more efficient in cancers with genetically activated *MYC*.[48] Although it is understandable why *BRG1*-mutant cells are resistant to GC/RA-based treatments, the mechanism underlying the responsiveness of MYC-activated cancer cells to these treatment has yet to be identified. Supra-physiological levels of GC and/or RA may be required to compete with MYC to bind to the SWI/SNF complex, causing it to switch its activities from cell growth to cell differentiation (Figure 6f). The case of the A549 cells, which carry inactivated *BRG1* but undergo changes in cell morphology and whose levels of MYC are reduced when treated with GC/RA, is intriguing and needs further investigation.

Until now, little has been known about the effects of a combination of corticoids and/or retinoids with epigenetic drugs in lung cancer patients. HDAC inhibitors have been used in combination with ATRA to treat certain types of leukemia[21,25] and with corticoids in multiple myeloma and peripheral T-cell lymphoma patients.[48,49] Studies combining retinoids and HDAC inhibitors in a xenograft model of neuroblastoma revealed synergistic effects and increased survival.[50] We were unable to extrapolate to mouse models the enhanced effects on reduced cell growth after combining A/S and GC/RA. Additional *in vivo*

experiments assaying a range of drug concentrations and administration schedules are warranted. Assessing the possible benefits of combining GC/RA with other chemotherapeutic agents or vitamins/hormones would also be worthwhile.

Our current data indicate that treatments based on epigenetic drugs combined with GC/RA may provide an opportunity for treating lung cancer patients bearing tumors with *MYC* activation. A complete understanding of this genotype–therapeutic relationship should help clinicians select the patient cohorts most likely to respond to epigenetic drugs.

MATERIALS AND METHODS

Cell culture

All the cell lines were obtained from the American Type Culture Collection (ATCC, Rockville, MD, USA), except the HCC33 that came from the Leibniz Institute DSMZ-German Collection of Microorganisms and Cell Cultures (DSMZ, Braunschweig, Germany). Cells were grown under recommended conditions and maintained at 37 °C in a humidified atmosphere of 5% CO_2/95% air. All cell lines were routinely evaluated for mycoplasma contamination. The cell lines were authenticated by genotyping for *TP53* and other known mutations.[6] Genomic DNA and total RNA were extracted by standard protocols. The study was approved by the relevant institutional review boards and ethics committees.

IC_{50} and isobologram analysis

For the purpose of IC_{50} calculations, the combinations of each GC/RA and A/S were considered as a single drug. In brief, cells were treated with the various combinations for 96 h. Estimates of IC_{50} were derived from the dose–response curves. The isobologram analysis provides a graphical presentation of the nature of interaction of two drugs. First, in a two-coordinate plot with one coordinate representing concentration of azacytidine and the other representing concentration of SAHA, the line of additivity is constructed by connecting their respective IC_{50}, when used as single agents. Second, the concentrations of the two drugs used in combination to provide the same effect (IC_{50}) are placed in the same plot. Synergy, additivity or antagonism is indicated when this point is located below, on or above the line, respectively.

Antibodies and western blottings

The following primary antibodies were used for western blottings: polyclonal anti-BRG1, H88 (1:1000; Santa Cruz Biotechnology, Santa Cruz, CA, USA); anti-C-MYC, N-262 (1:500; Santa Cruz Biotechnology); anti-N-MYC, B8.4.B (1/500, Santa Cruz Biotechnology); anti-TUBULIN, T6199 mouse (1/10000, Sigma-Aldrich, St Louis, MO, USA); anti-Beta-ACTIN, 13854 (1/20000 Sigma-Aldrich); anti-Ki67, SP6 (1/100, Thermo Scientic, Waltham, MA, USA); anti-Caspase-3, 3G2 (1/2000, Cell Signalling); and anti-PARP, C2–10 (1/5000, BD Pharmingen, San Diego, CA, USA). For western blottings, whole-cell lysates were collected in a buffer containing 2% sodium dodecyl sulfate 50 mM Tris-HCl (pH 7.4), 10% glycerol and protease inhibitor cocktail (Roche Applied Science, Roche, Basel, Switzerland). Protein concentrations were determined using a Bio-Rad DC Protein Assay Kit (Life Science Research, Hercules, CA, USA). Equal amounts of lysates (20 µg) were separated by sodium dodecyl sulfate-polyacrylamide gel electrophoresis and transferred to a polyvinylidene difluoride membrane that was blocked with 5% nonfat dry milk. Membranes were incubated with the primary antibody overnight at 4 °C, then washed before incubation with species-appropriate horseradish peroxidase-conjugated secondary antibodies for 1 h at room temperature.

Cell treatments and short hairpin RNAs (shRNAs)

For GC and RA treatment, we used synthetic GC dexamethasone and all-*trans* RA, respectively; chemicals were obtained from the following sources: ATRA (Sigma Chemical Co., Zwijndrecht, The Netherlands); dexamethasone (Sigma Chemical); and azacitidine (Sigma Chemical), SAHA, suberoyl+anilide+hydroxamic acid (Cayman Chemical Company, Ann Arbor, MI, USA).

shRNAs against BRG1 were purchased from SIGMA-MISSION (LentiExpress Technology, Sigma-Aldrich) as a glycerol stock of five pLKO plasmids carrying BRG1-specific shRNA sequences. These shRNAs had previously been shown to deplete BRG1 expression efficiently and specifically (depleted BRG1 but not BRM expression).[5] A scramble shRNA (Sigma MISSION shRNA non-mammalian control SHC002) was used as a control. The lentiviruses were generated within the 293T packaging cells, as previously described.[6]

Cell viability assays (3-(4,5)-dimethylthiazol-2-yl)-2,5-diphenyltetrazolium bromide (MTT)

For cell viability assays, cell lines were incubated in 96-well plates. Prior to harvest, cells were treated for 24–72 h with the indicated concentrations of each compound or combinations. For the assays, 10 µl of a solution of 5 mg/ml MTT (Sigma Chemical Co.) was added. After incubation for 3 h at 37 °C, the medium was discarded, the formazan crystals that had formed were dissolved in 100 µl DMSO and absorbance was measured at 596 nm. Results are presented as the median of at least two independent experiments performed in triplicate for each cell line and for each condition.

Global gene expression and methylation microarray analysis

The cells used for microarray gene expression and methylation analysis were the MYC-amplified and BRG1 wild-type H82, H460 and the BRG1 mutant and MYC wild-type H1299, A549 and DMS114 cells. In all, 100 ng of RNA was used for the gene expression microarray analysis. Each of the cells were subjected to different treatments. Treatment with GC/RA (1 µM each) or with GC/RA/A/S (0.2 µM each) for 5 days. Untreated cells (fetal bovine serum) were included as a control. RNA integrity numbers were in the range of 9.0–10.0 when assayed by Lab-chip Technology in an Agilent 2100 Bioanalyzer (Agilent, Santa Clara, CA, USA). For labeling, we used a commercial 'One-Color Microarray-Based Gene Expression Analysis' version 5.5 kit and followed the manufacturer's instructions (Agilent manual G4140-90050 (Agilent), February 2007). Hybridization was performed on the Human Gene Expression v2 microarray 8x60K (Agilent microarray design ID 014850, P/N G4112F, Agilent). For scanning, we used a G2505B DNA microarray scanner. Images were quantified using the Agilent Feature Extraction Software (v.9.5, Agilent). Data were read, preprocessed and analyzed using limma package in the R/Bioconductor environment. For hierarchical clustering of samples, we used the most 10 000 dynamic probes. To generate the lists of upregulated and downregulated transcripts for each condition, we chose transcripts induced or repressed by a factor of at least two for each treatment relative to their matched cell line untreated and statistical significance (*P*-adjusted value < 0.05). The genes are listed in Supplementary Tables S2–S5.

For DNA methylation microarrays, all DNA samples were assessed for integrity, quantity and purity by electrophoresis in a 1.3% agarose gel, PicoGreen quantification (Thermo Scientific, Willmngton, DE, USA) and NanoDrop measurement (Thermo Scientific). We performed bisulfite conversion of 500 ng of genomic DNA using an EZ DNA Methylation Kit (Zymo Research, Orange, CA, USA). Bisulfite-converted DNA (200 ng) was used for hybridization on the HumanMethylation450 BeadChip (Illumina, San Diego, CA, USA). Raw fluorescence intensity values were normalized with the Illumina Genome Studio software (V2011.1) using 'control normalization' with background correction. Normalized intensities were then used to calculate DNA methylation levels (beta values). Likewise, data points with statistically low power (as reported by detection values of $P > 0.01$) were designated as NA and excluded from the analysis. Genotyping probes present on the chip and DNA methylation probes overlapping with known single-nucleotide polymorphisms were also removed. Probes were considered to be in a promoter CpG island if they were located within a CpG island (UCSC database) and < 2000 bp away from a transcription start site (outside chromosome X). We only considered CpG sites with a $\geqslant 70\%$ change in CpG methylation level between primary and metastases sites, and the differential CpG methylation primary and metastasis had to occur in the three tumor types studied. Samples were clustered in an unsupervised manner by using the 10 000 most variable values for CpG methylation according to the s.d. for the CpG sites located in promoter regions by hierarchical clustering using the complete method for agglomerating the Manhattan distances.

Orthotopic xenograft models

Athymic mice male nu/nu aged 4–5 weeks were maintained in a sterile environment. All animal specimens used for the experiments were male. None of the mice samples were excluded before analysis. All animal experiments were approved by the IDIBELL Ethical Committee

(no. AAALAC-3880) and performed in accordance with guidelines stated in The International Guiding Principles for Biomedical Research involving Animals, developed by the Council for International Organizations of Medical Sciences.

The different lung cancer cell lines (2×10^6) were first grown subcutaneously and then implanted orthotopically into the lung. Once the tumor had grown to 600–800 mm^3, it was cut into 3×3 mm^2 pieces and maintained in Dulbecco's modified Eagle's medium supplemented medium with 10% fetal bovine serum and penicillin/streptomycin. Those fragments with macroscopically low or absent levels of necrotic areas were selected for orthotopic implantation No randomization of animals was performed, but animals were age matched, and littermates were used whenever possible.

Animals were treated by intraperitoneal injection with all-*trans* RA plus dexamethasone (GC) (2.5 mg/kg/day each), azacitidine plus SAHA (2.5 mg/kg/day each) and cisplatin (cis) (4.5 mg/kg/day) in different combination of the various treatments or corresponding vehicle only. The treatments were initiated from 8 to 10 days after tumor implantation. Each treatment was administrated weekly for 3 weeks (Supplementary Table S7).

Animals were killed when they displayed serious respiratory difficulty, which was subsequently confirmed to be associated with lung tumor burden. For histological analysis of lung tumors, lungs were fixed and embedded in paraffin. Necrosis was morphologically assessed after staining with hematoxilin and eosin, using standard protocols, and examined by light microscopy in a blinded manner. For Ki67 immunohistochemical staining, 4 μm thick sections from the tumors were transferred to silanized glass slides. After deparaffinization and quenching endogenous peroxidase, the slides were boiled in citrate buffer for 15 min. After antibody incubation, immunodetection was performed with the secondary anti-rabbit-conjugated horseradish peroxidase (Dako, Glostrup, Denmark) with diaminobenzidine chromogen as the substrate (Invitrogen, Carlsbad, CA, USA). Sections were counterstained with hematoxylin and evaluated with the Leica DM1000 microscope (Leica, Wetzlar, Germany). Criteria for evaluating Ki67 immunostaining was the percentage of positively stained nuclei relative to total nuclei.

Statistical analysis

Numerical values are reported as average ± s.d. unless stated otherwise. Data are derived from multiple independent experiments from distinct mice or cell culture plates, unless stated otherwise. No statistical method was used to predetermine sample size, but sample size was based on preliminary data and previous publications as well as observed effect sizes.

We assessed data for normal distribution and similar variance between groups using GraphPad Prism 6.0 (San Diego, CA, USA), if applicable. Some data sets had a statistical difference in the variation between groups. Data were analyzed using a one-way analysis of variance or a two-tailed Student's unpaired-samples *t*-test, as appropriate. Differences were considered statistically significant for values of $P < 0.05$.

Kaplan–Meier estimates of the survival distribution for each group were computed. Survival analysis was performed in Graphpad Prism, survival curves being compared by the log-rank (Mantel–Cox) test. In order to test the equality of the survival distributions for different groups, the log rank was calculated. We considered groups to have significantly different survival distributions if the test result yielded a value of $P < 0.05$.

Accession code

Microarray gene expression and methylation data are available in the Gene Expression Omnibus (GEO) under accession code GSE66245.

CONFLICT OF INTEREST

The authors declare no conflict of interest.

ACKNOWLEDGEMENTS

We thank Patricia Cabral (Genes and Cancer Group) at IDIBELL for technical assistance. This work was supported by the grants from the Spanish MINECO SAF2011-22897, Institute of Health Carlos III (ISCIII)-PIE13/00022 (ONCOPROFILE) and RTICC (RD12/0036/0045 to MS-C and RD12/0036/0039 to ME) and a grant from the Fundación Científica Asociacion Española Contra el Cáncer-GCB14-2170. MT-D is supported by a fellowship from the Spanish MINECO. Funding was also provided by the European Union Seventh Framework Programme (FP7/2007-13), under grant agreement HEALTH-F2-2010-258677–CURELUNG.

AUTHOR CONTRIBUTIONS

OAR, MT-D and SV performed and analyzed most of the experiments. SM performed the DNA methylation microarrays. AG and SM analyzed the bioinformatic data. SV and EC performed and analyzed the histopathological work. AV generated the mouse models and designed/supervised the mouse work. ME supervised the global DNA methylation analysis. OAR and MS-C designed the overall study. MS-C supervised the research and wrote the manuscript. All authors discussed the results and commented on the manuscript.

REFERENCES

1 Wilson GB, Roberts CWM. SWI/SNF nucleosome remodellers and cancer. *Nat Rev Cancer* 2011; **11**: 481–492.
2 Romero OA, Sanchez-Cespedes M. The SWI/SNF genetic blockade: effects in cell differentiation, cancer and developmental diseases. *Oncogene* 2014; **33**: 2681–2689.
3 Medina PP, Romero OA, Kohno T, Montuenga LM, Pio R, Yokota J, Sanchez-Cespedes M. Frequent BRG1/SMARCA4-inactivating mutations in human lung cancer cell lines. *Hum Mutat* 2008; **29**: 617–622a.
4 Rodriguez-Nieto S, Cañada A, Pros E, Pinto AI, Torres-Lanzas J, Lopez-Rios F *et al.* Massive parallel DNA pyrosequencing analysis of the tumor suppressor BRG1/SMARCA4 in lung primary tumors. *Hum Mutat* 2011; **32**: E1999–E2017.
5 Romero OA, Setien F, John S, Gimenez-Xavier P, Gómez-López G, Pisano D *et al.* The tumour suppressor and chromatin-remodelling factor BRG1 antagonizes Myc activity and promotes cell differentiation in human cancer. *EMBO Mol Med* 2012; **4**: 603–616.
6 Romero OA, Torres-Diz M, Pros E, Savola S, Gomez A, Moran S *et al.* MAX inactivation in small cell lung cancer disrupts MYC-SWI/SNF programs and is synthetic lethal with BRG1. *Cancer Discov* 2014; **4**: 292–303.
7 Cheng SW, Davies KP, Yung E, Beltran RJ, Yu J, Kalpana GV. c-MYC interacts with INI1/hSNF5 and requires the SWI/SNF complex for transactivation function. *Nat Genet* 1999; **22**: 102–105.
8 Pal S, Yun R, Datta A, Lacomis L, Erdjument-Bromage H, Kumar J *et al.* mSin3A/histone deacetylase 2- and PRMT5-containing Brg1 complex is involved in transcriptional repression of the Myc target gene cad. *Mol Cell Biol* 2003; **23**: 7475–7487.
9 Peterson CL, Dingwall A, Scott MP. Five SWI/SNF gene products are components of a large multisubunit complex required for transcriptional enhancement. *Proc Natl Acad Sci USA* 1994; **91**: 2905–2908.
10 Kwon H, Imbalzano AN, Khavari PA *et al.* Nucleosome disruption and enhancement of activator binding by a human SW1/SNF complex. *Nature* 1994; **370**: 477–481.
11 De la Serna IL, Carlson KA, Imbalzano AN. Mammalian SWI/SNF complexes promote MyoD-mediated muscle differentiation. *Nat Genet* 2001; **27**: 187–190.
12 Seo S, Richardson GA, Kroll KL. The SWI/SNF chromatin remodeling protein Brg1 is required for vertebrate neurogenesis and mediates transactivation of Ngn and NeuroD. *Development* 2005; **132**: 105–151.
13 Chi TH, Wan M, Lee PP, Akashi K, Metzger D, Chambon P *et al.* Sequential roles of Brg, the ATPase subunit of BAF chromatin remodeling complexes, in thymocyte development. *Immunity* 2003; **19**: 169–182.
14 Chiba H, Muramatsu M, Nomoto A, Kato H. Two human homologues of *Saccharomyces cerevisiae* SWI2/SNF2 and Drosophila brahma are transcriptional coactivators cooperating with the estrogen receptor and the retinoic acid receptor. *Nucleic Acids Res* 1994; **22**: 1815–1820.
15 Ostlund Farrants AK, Blomquist P, Kwon H, Wrange O. Glucocorticoid receptor-glucocorticoid response element binding stimulates nucleosome disruption by the SWI/SNF complex. *Mol Cell Biol* 1997; **17**: 895–905.
16 Fryer CJ, Archer TK. Chromatin remodelling by the glucocorticoid receptor requires the BRG1 complex. *Nature* 1998; **393**: 88–91.
17 Flajollet S, Lefebvre B, Cudejko C, Staels B, Lefebvre P. The core component of the mammalian SWI/SNF complex SMARCD3/BAF60c is a coactivator for the nuclear retinoic acid receptor. *Mol Cell Endocrinol* 2007; **270**: 23–32.
18 Johnson TA, Elbi C, Parekh BS, Hager GL, John S. Chromatin remodeling complexes interact dynamically with a glucocorticoid receptor-regulated promoter. *Mol Biol Cell* 2008; **19**: 3308–3322.
19 Maeda Y, Davé V, Whitsett JA. Transcriptional control of lung morphogenesis. *Physiol Rev* 2007; **87**: 219–244.

20 Sionov RV, Spokoini R, Kfir-Erenfeld S, Cohen O, Yefenof E. Mechanisms regulating the susceptibility of hematopoietic malignancies to glucocorticoid-induced apoptosis. *Adv Cancer Res* 2008; **101**: 127–248.
21 Schenk T, Stengel S, Zelent A. Unlocking the potential of retinoic acid in anticancer therapy. *Br J Cancer* 2014; **111**: 2039–2045.
22 Collins SJ. The role of retinoids and retinoic acid receptors in normal hematopoiesis. *Leukemia* 2002; **16**: 1896–1905.
23 Rutz HP. Effects of corticosteroid use on treatment of solid tumours. *Lancet* 2002; **360**: 1969–1970.
24 Pottier N, Yang W, Assem M, Panetta JC, Pei D, Paugh SW *et al.* The SWI/SNF chromatin-remodeling complex and glucocorticoid resistance in acute lymphoblastic leukemia. *J Natl Cancer Inst* 2008; **100**: 1792–1803.
25 Siegel D, Hussein M, Belani C, Robert F, Galanis E, Richon VM *et al.* Vorinostat in solid and hematologic malignancies. *J Hematol Oncol* 2009; **2**: 31.
26 Liu SV, Fabbri M, Gitlitz BJ, Laird-Offringa IA. Epigenetic therapy in lung cancer. *Front Oncol* 2013; **3**: 135.
27 Vendetti FP, Rudin CM. Epigenetic therapy in non-small-cell lung cancer: targeting DNA methyltransferases and histone deacetylases. *Expert Opin Biol Ther* 2013; **13**: 1273–1285.
28 Juergens RA, Wrangle J, Vendetti FP, Murphy SC, Zhao M, Coleman B *et al.* Combination epigenetic therapy has efficacy in patients with refractory advanced non-small cell lung cancer. *Cancer Discov* 2011; **1**: 598–607.
29 McDermott U, Sharma SV, Dowell L, Greninger P, Montagut C, Lamb J *et al.* Identification of genotype-correlated sensitivity to selective kinase inhibitors by using high-throughput tumor cell line profiling. *Proc Natl Acad Sci USA* 2007; **104**: 19936–19941.
30 Facchini LM, Chen S, Marhin WW, Lear JN, Penn LZ. The Myc negative autoregulation mechanism requires Myc-Max association and involves the c-myc P2 minimal promoter. *Mol Cell Biol* 1997; **17**: 100–114.
31 Sivak LE, Tai KF, Smith RS, Dillon PA, Brodeur GM, Carroll WL. Autoregulation of the human N-myc oncogene is disrupted in amplified but not single-copy neuroblastoma cell lines. *Oncogene* 1997; **15**: 1937–1946.
32 Borczuk AC, Gorenstein L, Walter KL, Assaad AA, Wang L, Powell CA. Non-small-cell lung cancer molecular signatures recapitulate lung developmental pathways. *Am J Pathol* 2003; **163**: 1949–1960.
33 Angulo B, Suarez-Gauthier A, Lopez-Rios F, Medina PP, Conde E, Tang M *et al.* Expression signatures in lung cancer reveal a profile for EGFR-mutant tumours and identify selective PIK3CA overexpression by gene amplification. *J Pathol* 2008; **214**: 347–356.
34 Castillo SD, Matheu A, Mariani N, Carretero J, Lopez-Rios F, Lovell-Badge R *et al.* Novel transcriptional targets of the SRY-HMG box transcription factor SOX4 link its expression to the development of small cell lung cancer. *Cancer Res* 2012; **72**: 176–186.
35 Bogue CW, Gross I, Vasavada H, Dynia DW, Wilson CM, Jacobs HC. Identification of Hox genes in newborn lung and effects of gestational age and retinoic acid on their expression. *Am J Physiol* 1994; **266**: L448–L454.
36 Sandoval J, Heyn H, Moran S, Serra-Musach J, Pujana MA, Bibikova M. Validation of a DNA methylation microarray for 450,000 CpG sites in the human genome. *Epigenetics* 2011; **6**: 692–702.
37 Bibikova M, Barnes B, Tsan C, Ho V, Klotzle B, Le JM *et al.* High density DNA methylation array with single CpG site resolution. *Genomics* 2011; **98**: 288–295.
38 Bonastre E, Verdura S, Zondervan I, Facchinetti F, Lantuejoul S, Chiara MD *et al.* PARD3 inactivation in lung squamous cell carcinomas impairs STAT3 and promotes malignant invasion. *Cancer Res* 2015; **75**: 1287–1297.
39 Saffiotti U, Montesano R, Sellakumar AR, Borg SA. Experimental cancer of the lung. Inhibition by vitamin A of the induction of tracheobronchial squamous metaplasia and squamous cell tumors. *Cancer* 1967; **20**: 857–864.
40 Malpel S, Mendelsohn C, Cardoso WV. Regulation of retinoic acid signaling during lung morphogenesis. *Development* 2000; **127**: 3057–3067.
41 Shi W, Chen F, Cardoso WV. Mechanisms of lung development contribution to adult lung disease and relevance to chronic obstructive pulmonary disease. *Proc Am Thorac Soc* 2009; **6**: 558–563.
42 Greenberg AK, Hu J, Basu S, Hay J, Reibman J, Yie TA *et al.* Glucocorticoids inhibit lung cancer cell growth through both the extracellular signal-related kinase pathway and cell cycle regulators. *Am J Respir Cell Mol Biol* 2002; **27**: 320–328.
43 Geradts J, Chen JY, Russell EK, Yankaskas JR, Nieves L, Minna JD. Human lung cancer cell lines exhibit resistance to retinoic acid treatment. *Cell Growth Differ* 1993; **4**: 799–809.
44 Thulasi R, Harbour DV, Thompson EB. Suppression of c-myc is a critical step in glucocorticoid-induced human leukemic cell lysis. *J Biol Chem* 1993; **268**: 18306–18312.
45 Nagl Jr NG, Zweitzig DR, Thimmapaya B, Beck Jr GR, Moran E. The c-myc gene is a direct target of mammalian SWI/SNF-related complexes during differentiation-associated cell cycle arrest. *Cancer Res* 2006; **66**: 1289–1293.
46 Delmore JE, Issa GC, Lemieux ME, Rahl PB, Shi J, Jacobs HM *et al.* BET bromodomain inhibition as a therapeutic strategy to target c-Myc. *Cell* 2011; **146**: 904–917.
47 Sharm SV, Settleman J. Oncogene addiction: setting the stage for molecularly targeted cancer therapy. *Genes Dev* 2007; **21**: 3214–3231.
48 San-Miguel JF, Hungria VT, Yoon SS, Beksac M, Dimopoulos MA, Elghandour A *et al.* Panobinostat plus bortezomib and dexamethasone versus placebo plus bortezomib and dexamethasone in patients with relapsed or relapsed and refractory multiple myeloma: a multicentre, randomised, double-blind phase 3 trial. *Lancet Oncol* 2014; **15**: 1195–1206.
49 Hopfinger G, Nösslinger T, Lang A, Linkesch W, Melchardt T, Weiss L *et al.* Lenalidomide in combination with vorinostat and dexamethasone for the treatment of relapsed/refractory peripheral T cell lymphoma (PTCL): report of a phase I/II trial. *Ann Hematol* 2014; **93**: 459–462.
50 Hahn CK, Ross KN, Warrington IM, Mazitschek R, Kanegai CM, Wright RD *et al.* Expression-based screening identifies the combination of histone deacetylase inhibitors and retinoids for neuroblastoma differentiation. *Proc Natl Acad Sci USA* 2008; **105**: 9751–9756.

Supplementary Information accompanies this paper on the Oncogene website (http://www.nature.com/onc)